Carbohydrate Polymers 98 (2013) 80–88

Contents lists available at SciVerse ScienceDirect

Carbohydrate Polymers

journal homepage: www.elsevier.com/locate/carbpol

Synthesis of HPMC stabilized nickel nanoparticles and investigation of their magnetic and catalytic properties

Dipanwita Maity[a], Md. Masud Rahaman Mollick[a], Dibyendu Mondal[a], Biplab Bhowmick[a], Swarup Kumar Neogi[b], Aritra Banerjee[b], Sanatan Chattopadhyay[c], Sudipta Bandyopadhyay[b,*], Dipankar Chattopadhyay[a,*]

[a] Department of Polymer Science and Technology, University College of Science and Technology, University of Calcutta, 92 A.P.C. Road, Kolkata 700009, India
[b] Department of Physics, University of Calcutta, 92 A.P.C. Road, Kolkata 700009, India
[c] Department of Electronic Science, University of Calcutta, 92 A.P.C. Road, Kolkata 700009, India

ARTICLE INFO

Article history:
Received 14 February 2013
Received in revised form 5 April 2013
Accepted 11 May 2013
Available online 31 May 2013

Keywords:
Nickel nanoparticles
Hydroxypropylmethylcellulose
Magnetic material
Suzuki coupling reaction

ABSTRACT

Nickel nanoparticles synthesized from $NiCl_2 \cdot 6H_2O$ by hydrazine hydrate in mixed solvent of ethanol and water in the presence of hydroxypropylmethylcellulose (HPMC) as protective and stabilizing agents. The morphology and sizes of synthesized Ni nanoparticles were studied by field-emission-scanning-electron microscopy (FESEM). Structural properties of nanoparticles were examined by X-ray diffraction (XRD). The polymer stabilized Ni nanoparticles were characterized by Fourier-transform infrared (FTIR) spectroscopy. The magnetic measurement showed that the resultant Ni nanoparticles were ferromagnetic. Also, the saturation magnetization (M_S), remanent magnetization (M_R) and coercivity (M_R) were observed to increase with decreasing temperature. The results of magnetic characterization showed that the magnetic properties of the HPMC stabilized Ni nanoparticles are quite different from those of the bared Ni nanoparticles. All the observed magnetic properties essentially reflected the very typical nanoparticle type nature. Consequently, the resulting Ni nanoparticles were found to be highly active and recyclable catalyst for Suzuki coupling reactions.

1. Introduction

Nano-structured magnetic materials have drawn our interest because of their novel physico-chemical properties and unique applications in diverse areas such as catalysis (Ferrando, Jellinek, & Johnston, 2008; H.X. Li, Zhao, Wan, Dai, & Qiao, 2006; Y. Li, Cai, Rogers, Xu, & Shen, 2006; Wu, Zhang, Zhao, Li, & Tao, 2008), data storage (Reiss & Hütten, 2005), sensors (Sadek et al., 2010) and medical diagnosis (Hernandez, Polizu, Turenne, & Yahia, 2002). Among these magnetic nanomaterials, a recent surge of interest is grown up for Ni nanoparticles due to their frequent exploitation in different synthetic and catalytic activity. Compared to traditional Raney Ni, these Ni nanoparticles have shown tremendous catalytic activity, feasible processability, ease of preparation, high stability and ease of recyclability, so forth, these are upcoming as an attractive area of research in the coming future. The magnetic as well as catalytic properties of Ni nanoparticles are strongly dependent on the morphology and shape of the nanoparticles (Cordente et al., 2001; Kim, Lee, Choi, Park, & Park, 2004). Various attempts have been made to prepare Ni nanoparticles, e.g. wet chemical reduction in aqueous solution (Kim et al., 2005; Ni, J. Zhang, Zhang, & Zheng, 2007; Ni, Y.F. Zhang, Song, & Zheng, 2007; Wang, Sun, Yu, & Meng, 2008; Wu & Chen, 2004) or in organic media (Alonso, Calvino, Osante, & Yus, 2005; Bai, Yuan, & Tang, 2008; Couto et al., 2007; Hou & Gao, 2003; Jiang, Xie, Jiang, Jing, & Qin, 2012; Yu, Kim, Chung, & Liang, 2003), microemulsion (Chen & Wu, 2000; Zhang et al., 2005), hydrothermal techniques (Wang et al., 1998), electrical method (Zach & Penner, 2000), metal salt reduction (Hou & Gao, 2003), ultrasound-spray pyrolysis (Stopic, Nedeljkovic, Rakocevic, & Uskokovic, 1999), polyol method (Carroll, Reveles, Shultz, Khanna, & Carpenter, 2011) and neutral organometallic precursor decomposition (Park et al., 2005; Zhang, Wu, Chen, & Qui, 2006). Chemical reduction method has the advantage of simplicity, precise control of the size and low cost compared with the existing physical methods. Although the wet chemical reduction has its own simplicity but it is hard to get phase pure Ni nanoparticles in aqueous media because the oxidation of these nanoparticles facilitates in the aqueous media (Chen & Hsieh, 2002; H.X. Li et al., 2006; Y. Li et al., 2006) which renders their application. The phase pure Ni nanoparticles were synthesized in organic solvents like tetrahydrofuran (Domínguez-Crespo, Ramírez-Meneses, Montiel-Palma, Torres Huerta, & Dorantes Rosales, 2009), hexadecylamine

* Corresponding authors. Tel.: +91 9433379034; fax: +91 33 23519755.
E-mail address: dipankar.chattopadhyay@gmail.com (D. Chattopadhyay).

0144-8617/$ – see front matter © 2013 Elsevier Ltd. All rights reserved.
http://dx.doi.org/10.1016/j.carbpol.2013.05.020

(Hou & Gao, 2003), ethylene glycol (Yu et al., 2003) and ethanol (Bai et al., 2008) in order to avoid the oxidation of Ni nanoparticles. Ethanol was used as solvent and played the complementary reducing role. The difficulty with these magnetic nanoparticles is their tendency to agglomerate due to magnetic dipole–dipole attractions in order to reduce their surface energy. An important feature in the production of nanoparticles is the ability to keep them physically separated from each other preventing irreversible aggregation. The aggregation of nanoparticles can be eliminated by steric (coating the particles with a steric stabilizer layer) or ionic (inducing opposite charge on the particle surface) repulsion (Brust, Walker, Bethell, Schiffrin, & Whyman, 1994; Couto et al., 2007; Oliveira, Zanchet, Ugrate, & Zarbin, 2005).

Reported literature stated that several organic modifiers, such as tetrabutyl ammonium bromide (Chen & Hsieh, 2002; Singla, Negi, Mahajan, Singh, & Jain, 2007) sulfonated polybutadiene (Jiang et al., 2012) and cetyltrimethylammonium bromide (Abdel-Aal, Malekzadeh, Rashad, El-Midany, & El-Shall, 2007) were used to prevent irreversible aggregation of magnetic nanoparticles. The surface coating does not only protect the particles from aggregation, but it can also affect their size, shape, polydispersity and the total effective moment of the nanoparticles (Shen, Laibinis, & Hatton, 1999). Generally the nanocrystallites are the outcome in precipitation technique but such dispersions are inherently unstable because the so-formed nanoscale crystallites are prone to aggregate themselves to form larger particles due to the presence of dipolar interactions among the magnetic nanoparticles. In this prospect, Jongen et al. synthesized copper oxalate particles of different shape and morphology of the crystallites in the presence of hydroxypropylmethylcellulose (HPMC) and they concluded that the concentration of HPMC has a distinct role in controlling the crystallite shape and morphology (Jongen, Bowen, Lemaitre, Valmalette, & Hofmann, 2000). Xiaomin Ni and coworkers reported the formation of chain like nickel wire by self-assembly of small nickel crystallites (Ni, J. Zhang et al., 2007; Ni, Y.F. Zhang et al., 2007). Wu et al. fabricated Ni nanoparticles by hydrazine reduction of nickel chloride in ethylene glycol at 60 °C without a protective agent (Wu & Chen, 2003). They proposed that sodium hydroxide (NaOH) used in this process is not only necessary to produce pure Ni but accelerates the reaction rate at an elevated temperature (60 °C) also. Roy et al. synthesized oxide-coated Ni nanoparticles with tetragonal crystalline structure by using borohydride reduction method (Roy, Srinivas, Ram, De Toro, & Mizutani, 2005). The effect of annealing in the as-prepared sample was efficient to observe fcc Ni peak and their subsequent ferromagnetic behavior. Also well dispersed Ni nanoparticles with uniform size were synthesized via a modified hydrazine reduction route without any surfactant by Bai et al. (2008). In the latest report, Rashid et al. reported polyvinyl methyl ether (PVME) assisted synthesis of chain-like cobalt–nickel alloy nanostructures and also investigated their magnetic and catalytic activity toward both organic and inorganic reactions in aqueous phase (Rashid, Raula, & Mandal, 2011).

The resulting nanoparticles exhibit a wide assortment of rich physical properties and may have potential applications in diverse areas. However, the effectiveness of their application will depend to a large extent on their stability against oxidation and obviously on their magnetic attributes. According to the reported literature the electronic and magnetic properties of the particles remains unaltered in the presence of the polymers as the extent of interaction of the polymers with the surface of the particles is very less (Roy et al., 2005; Singh & Srinivas, 2010). Such core–shell structures are of considerable interest for many applications, which require nanoparticles to have high magnetic susceptibility. The metallic magnetic component shows the magnetic sensitivity for interaction with the external field whereas the coating would provide a surface that could easily be functionalized. The magnetic properties of these magnetic nanomaterials strictly depend on the crystal structure with various morphologies obtained via different existing synthetic processes. Recently, Singh et al. synthesized bared and polymer coated tetragonal Ni nanoparticles by borohydride reduction method, and investigated their structural and anomalous magnetic properties (Singh & Srinivas, 2010). Y. Chen et al. observed that magnetization of the fcc Ni nanoparticles increases rapidly with saturation at around 10 kOe field, whereas that of hcp Ni nanoparticles increases slowly with no saturation even at 50 kOe (Chen, Peng, Lin, & Luo, 2007). N. Cordente et al. studied the magnetic properties of fcc Ni with various structural morphologies and concluded that the amine-capped structures had magnetization values comparable to the corresponding nickel 'bulk' ones (Cordente et al., 2003).

Homogeneous catalysts have exhibited high activity and selectivity with special applications in asymmetric catalysis, although they are often expensive and their separation and reuse trouble some. In recent years, however, heterogeneous catalysis has experienced an enormous progress, with the catalysts being, in some cases, even more selective than their homogeneous counterparts. Moreover, heterogeneous catalysts are easy to separate and reuse, minimizing the presence of metal traces in the product, improving the handling and process control and therefore, reducing the overall costs.

Extremely small size and large surface to volume ratio of nanosized catalysts makes themselves an efficient element of heterogeneous catalysis in organic synthesis. Recently, there has been growing interest of Ni nanoparticles as catalyst offer great opportunities for a wide range of applications owing to their easy preparation, potent catalytic activity, possible process ability, high stability and ease of recyclability compared to traditional Raney Ni catalyst. Ni nanoparticles have been used as catalyst in organic synthesis and chemical manufacturing processes including the chemo selective oxidative coupling of thiols (Saxena, Kumar, & Mozumdar, 2007), reduction of aldehydes and ketones (Alonso, Riente, & Yus, 2008a; Alonso, Riente, & Yus, 2008b; Alonso, Riente, & Yus, 2008c) hydrogenation of olefins (Dhakshinamoorty & Pitchumani, 2008) and Hantzsch condensation for polyhydroquinoline derivatives (Sapkal, Shelke, Shingate, & Shingare, 2009). Recently, it has been proved that Ni nanoparticles are generally unstable, and the exploration of appropriate support for stabilizing catalytic nanoparticles is a key factor in their successful and wide applications in heterogeneous catalysis.

The future progress in nanotechnology will be dependent on polymer assisted nanotechnology because the polymer provides simple, ecologically friendly, cost-effective and multifunctional properties and applications of the products. The imperative challenge now for researchers and industry is to develop industrial methods for production of various types of polymer coated nanoparticles at affordable cost. To prevent the particles from coalescing, polymers have been commonly used to sterically protect the particles. One may hope that nanoparticles and polymer nanocomposites consisting of non-aggregated nanoparticles with tailored shape, size, low polydispersity, spatial arrangement and multifunctional properties will find many future applications, of which we cannot even guess today.

In the present study, we have found a reproducible one step in situ synthesis of Ni nanoparticles by chemical reduction of nickel chloride using hydrazine hydrate in aqueous-ethanol medium in the presence of hydroxypropylmethylcellulose (HPMC) as a stabilizer. We hypothesized that the HPMC stabilized Ni nanoparticles could be a better option for Suzuki coupling reactions over other investigated metal nanoparticles. In addition the magnetic property and efficient catalytic activity toward Suzuki coupling reaction of synthesized Ni nanoparticles was also investigated.

2. Experimental

2.1. Materials

A cellulose derivative, hydroxypropylmethylcellulose (viscosity 50 cPs) (HPMC) was obtained from Central Drug House (P) Ltd., India. Nickel chloride and hydrazine hydrate was reagent of E. Merck., India. Sodium hydroxide was purchased from Merck, India. Ethanol was acquired from Hong Yang Chemicals Corporation, China. Other chemicals, unless specified were of reagent grade and used without further purification. The water used through out this work was triple distilled water.

2.2. Synthesis of Ni nanoparticles

The Ni nanoparticles were synthesized from nickel chloride in water alcohol mixture (3:1). In a typical synthetic route, 0.2 M nickel chloride was added to various amount of hydroxypropylmethylcellulose (1 wt% and 2 wt%) solution. Then, the mixture was treated with the ultrasonic sound for 15 min to get homogeneous mixture. An appropriate amount of hydrazine hydrate (2 M) was added dropwise into the solution. The pH of the solution was maintained 12–12.5 by using appropriate amount of NaOH solution. The resulting mixture was ultrasonicated at 60 °C for 1 h. The solutions became black indicating that the nickel crystallites were formed. The precipitate was filtered off and washed with distilled water in sequence to washing out by product impurities. Then, the precipitate was washed with ethanol to control surface oxidation. Initially, the precipitate was dried at room temperature and then dried at 50 °C in vacuum oven. The whole synthesis procedure is shown in Fig. 1. The obtained samples were referred as polymer stabilized Ni nanoparticles. The pure Ni nanoparticles were also prepared without any protecting agent following the same procedure mentioned above. These nanoparticles will be referred as bared Ni nanoparticles in our future discussion.

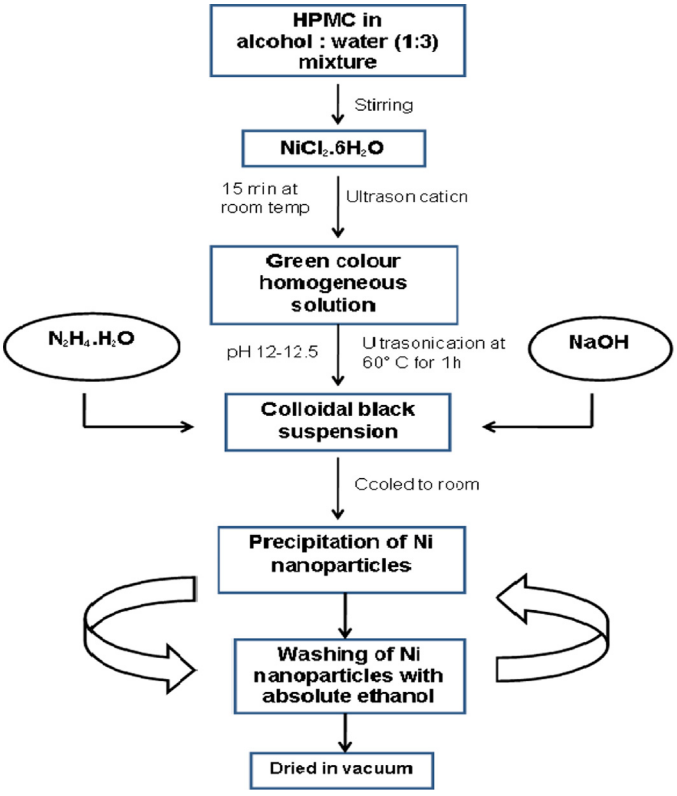

Fig. 1. Schematic diagram of synthesis of HPMC stabilized Ni nanoparticles.

2.3. General procedure for the Suzuki-coupling reactions

The Ni nanoparticles were employed as heterogeneous catalysts for Suzuki-coupling reaction (Table 2). In a typical run, an oven dried 10 mL round bottom flask was charged with a known mole percent of catalyst, cesium carbonate (Cs_2CO_3) (2.4 mmol), phenyl boronic acid (1.2 mmol) and aryl halide (1 mmol) in appropriate solvents (4 mL). The flask was placed in a preheated oil bath at required temperature. After the specified time, the flask was removed from the oil bath and water (20 mL) was added, followed by extraction with ether (4× 10 mL). The combined organic layers were washed with water (3× 10 mL), dried over anhydrous sodium sulphate and filtered. Solvent was removed under vacuum. The residue was dissolved in $CDCl_3$ and analyzed by ^1H NMR signal. Percent conversion was determined against the remaining aryl halide.

2.4. Characterization

The crystalline phase of the dried powder samples were analyzed by X-ray diffraction in a X-PERT-PRO Panalytical diffractometer at an accelerating voltage of 40 kV using Cu K_α ($\lambda = 1.5406$ Å) as X-ray source. Their size and morphology were inspected with field emission scanning electron microscopy (Zeiss Auriga, FESEM). For FTIR characterization, the sample pellets were first prepared by mixing the nanoparticles with KBr in a 1:100 (w/w) ratio. FTIR spectra were then acquired using this KBr pellet on a spectrophotometer (Shimadzu FTIR-8400S). The magnetic properties were investigated utilizing magnetic properties measurement system (MPMS) superconducting quantum interference device (SQUID) vibrating sample magnetometer (VSM). Field dependent magnetization (M-H) measurement was performed at 300 K, 200 K and 30 K for Ni nanoparticles and HPMC stabilized Ni nanoparticles. Temperature dependent magnetization (M-T) measurement was made under zero field cool (ZFC) and field cool (FC) conditions. The data was recorded in the heating cycle and temperature varies from 15 K to 300 K. M-T measurement under ZFC and FC conditions were performed at different magnetic fields of 100 Oe, 200 Oe, 500 Oe, 1000 Oe, 1500 Oe, 2500 Oe and 5000 Oe for Ni nanoparticles and HPMC stabilized Ni nanoparticles. ^1H NMR spectra were recorded on JEOL-ECS 400 MHz spectrometer.

3. Results and discussion

3.1. Formation of nickel nanoparticle

Nickel nanoparticles were synthesized by the reaction of a mixture of nickel (II) chloride in water alcohol mixture (3:1) with hydrazine hydrate at 60 °C by ultrasonic technique in the presence of hydroxypropylmethylcellulose (HPMC). The conventional reduction process of nickel using hydrazine hydrate as a reducing agent in the presence of NaOH was given in the literature as Eq. (1) (Li, Li, Wang, Li, & Qian, 1999) and Eq. (2) (Gao et al., 2001)

$$2[Ni(N_2H_4)_3]^{2+} + 4OH^- \rightarrow 2Ni(s) + N_2(g) + 4H_2O + 5N_2H_4 \quad (1)$$

$$2Ni(OH)_2 + N_2H_4 \rightarrow Ni + N_2 + 4H_2O \quad (2)$$

3.2. Structure and morphology of the HPMC stabilized nickel nanoparticles

XRD is employed to scrutinize the crystal phase as well as the crystal structure of the synthesized Ni nanoparticles. Fig. 2 shows

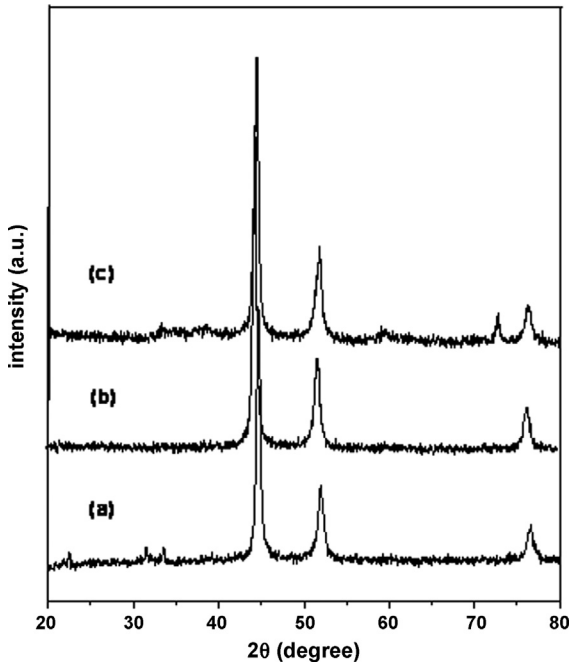

Fig. 2. XRD pattern of Ni nanoparticles synthesized (a) without stabilizing agent, (b) with 1 wt% HPMC and (c) with 2 wt% HPMC.

the XRD patterns of the Ni nanoparticles prepared in aqueous-alcohol medium both in the absence of protective agent (2a) and in the presence of 1 wt% and 2 wt% HPMC (2b and 2c) correspondingly. It is evident from the XRD pattern that both 2a and 2b consist of the diffraction peaks at $2\theta = 44.5^\circ$, 51.98° and 76.4° which are assigned to the crystal planes (1 1 1), (2 0 0) and (2 2 0) respectively. The obtained result implies that the as-synthesized Ni nanoparticles both in absence and in presence of 1 wt% HPMC exist in pure fcc structure (JCPDS card No. 04-0850). In these two patterns no peaks of hcp nickel are observed. On the contrary, at high concentration (2 wt%) of HPMC, Fig. 2(c) reveals the diffraction peaks at $2\theta = 38.5^\circ$, 58.9° and 72° corresponding to the crystal planes (0 1 0), (0 1 2), and (1 1 0) of hcp nickel (JCPDS No. 45-1027) along with the peaks of fcc nickel. So, we can conclude that the mixture comprises of nickel in both fcc and hcp crystalline structure in presence of 2 wt% HPMC. It is noticeable that the main peak, i.e. (1 1 1) plane of fcc nickel overlap with that of (0 1 1) plane of hcp nickel. These results designate that the low concentration of protective agent prefers the formation of fcc nickel whereas high concentration prefers formation of both fcc and hcp crystalline structure and also the sharp diffraction peak indicates adequate crystallinity of the synthesized Ni nanoparticles.

FESEM is employed in order to study the size and morphology of nickel nanoparticles and the recorded images are depicted in Fig. 3. It is quite clear from Fig. 3(a) and (b) that the spherical nickel nanoparticles with an average diameter of 250 nm are not well dispersed when prepared without using any stabilizing or protecting agent, i.e. HPMC. It is also clear from Fig. 3(c) and (d) (with 1 wt% HPMC) and Fig. 3(e) and (f) (with 2 wt% HPMC) that the nanoparticle morphology changes with change of HPMC concentration only. Fig. 3(c) and (d) shows well dispersed nickel nanospheres with mean diameter of 100 nm in presence of 1 wt% HPMC whereas Fig. 3(e) and (f) displays nanoflower like structure of nickel nanoparticles with some nanotips extending from the cores in presence of 2 wt% HPMC and also the nanoflowers form chain-like configuration which are fused into each other. So, it is obvious that there is a significant influence of the concentration of stabilizing or protective agent, i.e. HPMC on the resultant Ni nanoparticle morphology. Nickel nanoparticles with rough surfaces are spherical in presence of 1 wt% HPMC that is due to the insufficient stabilizer molecules adsorbed on the faces of nickel crystallite which, in turn, grows up to form spherical crystallite, followed by the aggregation to produce spherical nickel nanoparticles. It is understandable that the nanoparticle size should be decreased with increasing HPMC concentration owing to the higher absorption rate of stabilizer molecules. In contrast, the crystallite size increases with increase in HPMC concentration, which may contribute to the longer period for crystal growth. When the concentration of HPMC increases to 2 wt%, the growth rate of the face absorbed HPMC molecules is lower than that of the face without HPMC molecules. As a result, nickel crystallite will develop to give tip-like crystallite, afterward spherical nickel nanoparticles are formed by the aggregation of the tip-like crystallites.

3.3. FTIR analysis of HPMC stabilized nickel nanoparticles

The HPMC-stabilized nickel nanoparticles are further examined by FTIR analysis, as shown in Fig. 4. All the samples exhibit characteristics peaks for HPMC. The FTIR spectra of HPMC displays the peak at 3472 cm^{-1} attributing to –OH vibrational stretching shifted to 3458 cm^{-1} in HPMC stabilized Ni nanoparticles (Yao, Xu, Lu, & Deng, 2011). The band at 2917 cm^{-1} is assigned to the stretching of methyl and propyl group (Van der Weerd & Kazarian, 2005). The band between 1650 and 1600 cm^{-1} indicate the presence of stretching vibration of ν^{C-O} for six membered cyclic rings. The asymmetric bending vibrations of the methoxy group normally appear in the region 1500–1450 cm^{-1} whereas the range 1400–1350 cm^{-1} demonstrates the symmetric vibrations of methoxy group. The band between 1400 and 1350 cm^{-1} is liable for cyclic anhydrides. The band at 1100–1000 cm^{-1} reveals the stretching vibration of ethereal C—O—C groups and the band at 1000–950 cm^{-1} flaunts for the pyranose structure (Sahoo, Chakraborti, & Behra, 2012). All absorption bands in HPMC stabilized nanoparticles are shifted and also became broader. The broad absorption band in the 3400 cm^{-1} region represents hydrogen bonding in the polymer and absorbed water.

3.4. Magnetization study

The magnetic properties of the as synthesized nickel nanoparticles are studied by measuring both field dependent magnetization (M-H) and the temperature dependent magnetization (M-T) measurements. The variation of magnetization with magnetic field (M-H) at 30 K, 200 K and 300 K of bared and HPMC stabilized Ni nanoparticles have been shown in Fig. 5(a) and (b). All the variations clearly show expected nature of magnetic hysteresis which is indicative of ferromagnetic ordering. The parameters viz. saturation magnetization (M_S), remanent magnetization (M_R) and coercivity (H_C) of this sample at 30 K, 200 K and 300 K has been presented in Table 1. It is seen that the values of M_S, M_R and H_C are increased with decreasing temperature from 300 K to 30 K. This is due to the enhanced interactions of the spin magnetic moments which are quite regular and usual phenomenon for ferromagnetic system. This observed trend in HPMC stabilized Ni nanoparticles is quite similar with that of bared Ni nanoparticles sample. However, a careful inspection indicates some interesting dissimilarities for HPMC stabilized and bared Ni nanoparticles. M_S varies from 104 emu/g to 107 emu/g in case of bared Ni nanoparticles sample whereas for HPMC stabilized Ni nanoparticles sample it varies from 62 emu/g to 66 emu/g. The value of M_S is always higher for bared Ni nanoparticles sample. The values of M_S for the HPMC stabilized nanoparticles are found to be less than that of the bared nanoparticles which could be due to the nonmagnetic polymer coating and smaller particle size of the HPMC stabilized particles

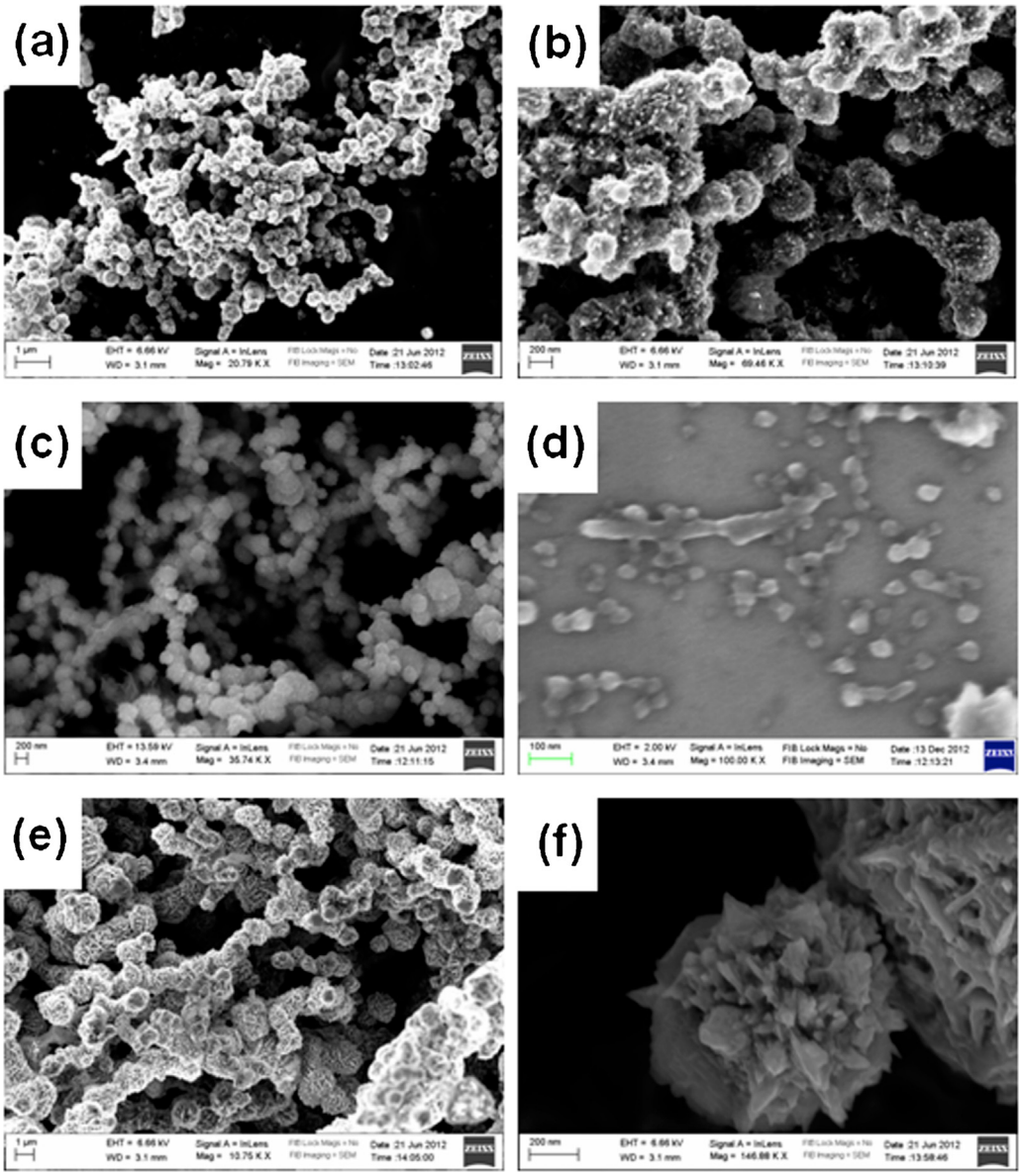

Fig. 3. FESEM images of (a and b) bare Ni nanoparticles synthesized without any stabilizing agent, (c and d) Ni nanoparticles synthesized with 1 wt% HPMC and (e and f) Ni nanoparticles synthesized with 2 wt% HPMC.

than that of the bared particles. M_R varies from 10 emu/g to 20 emu/g in case of bared Ni nanoparticles sample whereas for HPMC stabilized Ni nanoparticles sample it varies from 10 emu/g to 18 emu/g. The value of M_R is also higher for bared Ni nanoparticles sample at low temperature (i.e. 30 K). At 200 K the value of M_R is also still slightly higher for bared Ni nanoparticles sample. However, at room temperature (300 K) the value of M_R is more or less same for both varieties of samples; rather HPMC stabilized Ni nanoparticles sample shows a very slight higher value than its bared counterpart. H_C varies from 55 Oe to 162 Oe in case bared Ni nanoparticles sample whereas for HPMC stabilized Ni nanoparticles sample it varies from 133 Oe to 227 Oe. The value of H_C is always higher for HPMC stabilized Ni nanoparticles sample. It can be also seen that the hysteretic loop area for the HPMC stabilized nanoparticles is higher than that of the bared particles throughout the temperature range of 30–300 K (Fig. 5) and thus indicating the higher magnetic anisotropy and higher magnetic irreversibility of the HPMC stabilized nanoparticles than the bared nanoparticles.

The observation of more or less comparable value of M_R at room temperature and higher H_C values and simultaneous higher

Table 1
The values of saturation magnetization (M_S), remanent magnetization (M_R) and coercivity (H_C) of bared Ni and HPMC stabilized Ni at 30 K, 200 K and 300 K.

	30 K		200 K		300 K	
	Bared Ni	HPMC stabilized Ni	Bared Ni	HPMC stabilized Ni	Bared Ni	HPMC stabilized Ni
Saturation magnetization, M_S (emu/g)	106.6	66.3	104.0	64.7	104.0	62.0
Remanent magnetization, M_R (emu/g)	20.3	18.2	13.4	13.0	9.7	9.9
Coercivity, M_R (Oe)	162.0	226.6	88.0	132.5	55.0	94.0

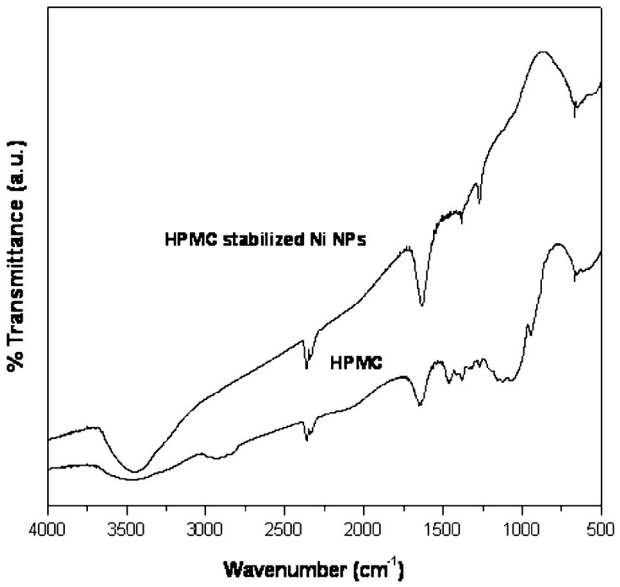

Fig. 4. FTIR spectra of pure HPMC and HPMC stabilized Ni nanoparticles.

ferromagnetic loop area throughout the temperature range of 30–300 K for HPMC stabilized Ni nanoparticles is really striking. Using polymer coating on Ni nanoparticles, the magnetic properties should be degraded and that is actually happening for saturation magnetization throughout the entire temperature range. The variation of M_R and H_C is indicative of revealing better magnetic properties for HPMC stabilized Ni nanoparticles at most crucial room temperature. Actually, low temperature magnetic properties studies of this kind of samples are generally performed to understand the underlying scientific mechanism prevailing in those systems. But, so far as their application potential particularly for surfactant property is concerned the most important is their role at room temperature. So the noteworthy point is that enhanced surfactant property shows by HPMC stabilized Ni nanoparticles are at least magnetically comparable (or rather may partially better) from their bared counterpart.

Temperature dependent magnetization (M-T) data were recorded in ZFC and FC conditions under different applied magnetic fields such as 100 Oe, 200 Oe, 500 Oe, 1000 Oe, 1500 Oe, 2500 Oe and 5000 Oe in the temperature region from 15 K to 300 K for both bared and HPMC stabilized Ni nanoparticle samples. M-T curves under ZFC and FC conditions for bared and HPMC stabilized Ni nanoparticle samples have been presented in Fig. 6. M-T curves under ZFC and FC conditions at the applied magnetic fields 100 Oe and 200 Oe indicate more or less similar nature for bared Ni nanoparticles [curves (i) and (ii) of Fig. 6(a)]. The magnetization under ZFC condition in these two cases monotonically increases with increasing temperature whereas magnetization under FC condition remains almost constant. The clear separation between magnetization curves under ZFC and FC conditions exist up to 300 K, indicating a blocking temperature above room temperature (Bai et al., 2008). Chen et al. also reported the same type of observation for fcc nickel (Chen et al., 2007). M-T curves under ZFC and FC conditions at the applied magnetic fields 100 Oe and 200 Oe indicate

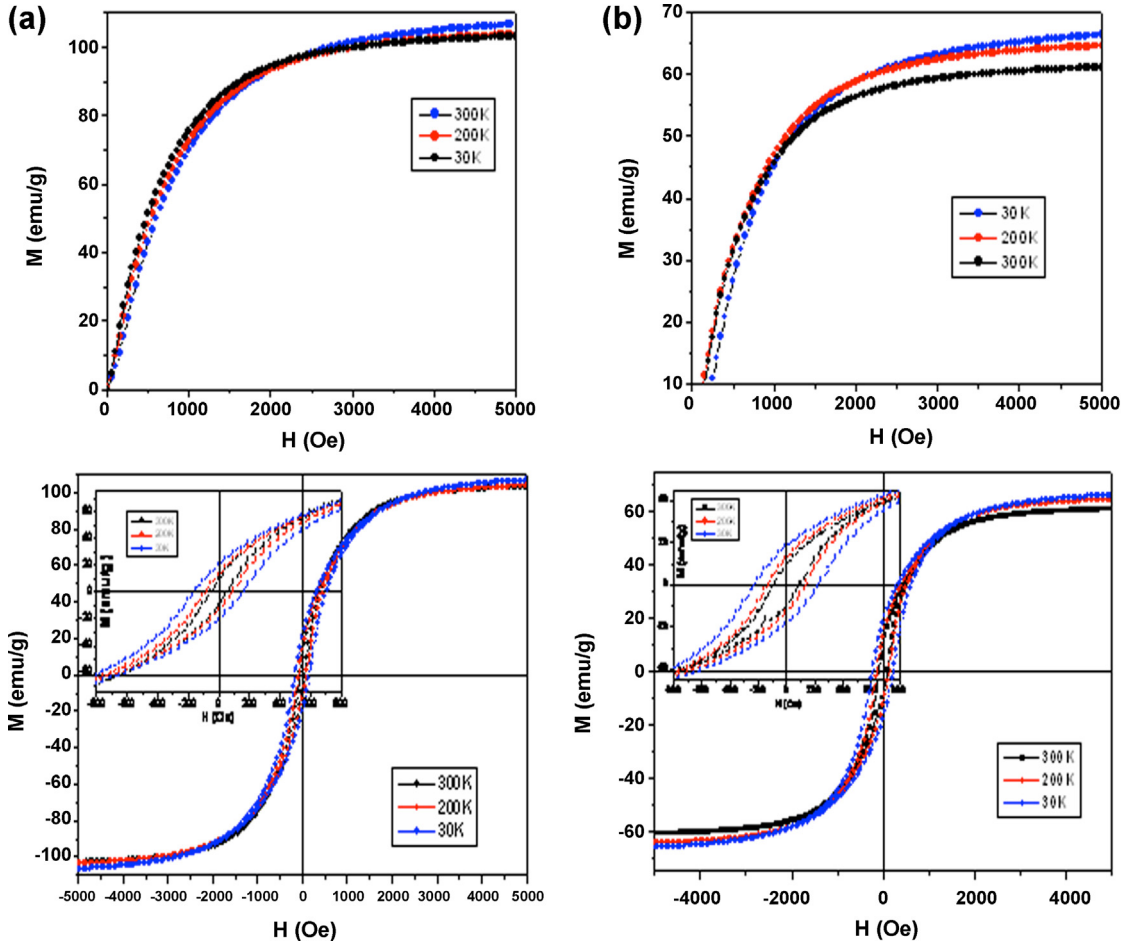

Fig. 5. *M–H* curves of (a) bared Ni and (b) HPMC stabilized Ni nanoparticles at different temperatures.

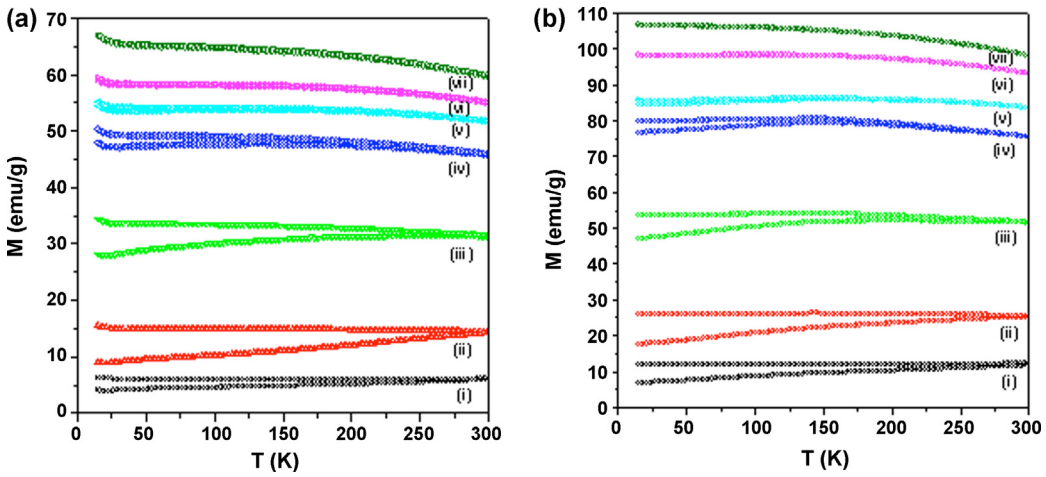

Fig. 6. Zero-field-cooled (ZFC) and field-cooled (FC) magnetization versus temperature curves of (a) bared and (b) HPMC stabilized nickel nanoparticles at applied magnetic field: (i) 100 Oe, (ii) 200 Oe, (iii) 500 Oe, (iv) 1000 Oe, (v) 1500 Oe, (vi) 2500 Oe and (vii) 5000 Oe.

more or less similar nature except in the low temperature regime of 15–25 K for HPMC stabilized Ni nanoparticles [curves (i) and (ii) of Fig. 6(b)]. In this low temperature regime (15–25 K) the magnetization curves under ZFC and FC conditions indicate decreasing trend with increasing temperature. But the trend for bared Ni nanoparticles M-T variation under ZFC and FC conditions at magnetic field 500 Oe and 1000 Oe is remarkably different [curves (iii) and (iv) of Fig. 6(a)]. All the four curves shows increasing trend of magnetization from 15 K to 150 K and after that it gradually decreases with increasing temperature. The separation between these magnetization curves at ZFC and FC conditions [curves (iii) and (iv) of Fig. 6(a)] decreases slightly in comparison to same variations taken at 100 Oe and 200 Oe [curves (i) and (ii) of Fig. 6(a)]. The most striking thing is that presence of nearly a peak in all of the curves as observed in Fig. 6(a) (iii) and (iv) is absent in Fig. 6(b) (iii) and (iv). So for HPMC stabilized Ni nanoparticles exhibit increasing trends for magnetization curve under ZFC condition at 500 Oe with increase in temperature. But the magnetization curve under ZFC condition at 1000 Oe show broad hump like feature. And magnetization curves under FC condition at 500 Oe and 100 Oe indicate decreasing trend with increase in temperature. Simultaneously the decreasing trend in magnetization in the low temperature regime [15–25 K] in all of the curves in HPMC stabilized Ni nanoparticles has also been observed as similar to Fig. 6(b) (i) and (ii). M-T variations under ZFC and FC conditions for higher fields such as 1500 Oe, 2500 Oe and 5000 Oe for bared Ni nanoparticles has been presented in Fig. 6(a) (v), (vi) and (vii). A clear separation between M-T curves under ZFC and FC conditions measured at 1500 Oe have been observed up to 175 K. After 175 K both the curves are merged [Fig. 6(a) (v)]. In case of M-T variations taken at higher fields 2500 Oe and 5000 Oe both magnetization curves under ZFC and FC conditions merged altogether throughout the entire temperature range [Fig. 6(a) (vi), (vii)]. It is quite expected. Actually the fields 2500 Oe and 5000 Oe are higher in comparison to the required field to attain M_S in the entire temperature range of 15–300 K. But in case of 1500 Oe field it is higher field with respect to the field to attain M_S at 300 K but is lower than M_S attaining field at 15 K. So at 1500 Oe field, merger of M-T curves under ZFC and FC conditions takes place around 175 K. M-T variations under ZFC and FC conditions for fields at 1500 Oe, 2500 Oe and 5000 Oe for HPMC coated Ni nanoparticles has been presented in Fig. 6(b) (v), (vi) and (vii). The features of these curves are similar to features of the curves 6(a) (v), (vi) and (vii) except in the low temperature regime [15–25 K], where decreasing trend of magnetization with increase in temperature has again been observed.

Actually the striking dissimilarities that has been observed between bared and HPMC stabilized Ni nanoparticles are as follows: the decreasing trend of M(T) in low temperature regime of 15–25 K with increase in temperature for HPMC stabilized Ni nanoparticles is totally absent in bared Ni nanoparticles. Secondly, a distinct peak like feature has been observed in M(T) curves for bared Ni nanoparticles around 150 K at measuring magnetic field of 500 Oe and 1000 Oe only. No such peak has been detected in any M-T variations for HPMC stabilized Ni nanoparticles. Beside, the absolute values of magnetization is slightly less in case of HPMC stabilized Ni nanoparticles in comparison to their bared Ni nanoparticles counterpart. It is expected due to coating of nonmagnetic polymer and smaller particle size in HPMC stabilized Ni nanoparticles.

3.5. *Catalytic activity of Ni nanoparticle for Suzuki coupling reactions*

Colloidal metal nanoparticles have attracted a lot of attention as catalyst for many organic reactions, because they have a characteristic high surface-to-volume ratio and consequently, a large fraction of the metal atoms are located at the surface and thus available for catalysis. The fact, that copper(I) species have started receiving attention as inexpensive catalysts for bringing about Suzuki type C–C cross coupling reactions, has prompted us to explore such catalytic properties in the Ni. The catalytic activity has been examined for Suzuki type coupling of phenylboronic acid and aryl halides to yield the biphenyl product. Six different aryl halides (*viz. p*-haloacetophenone (halo = chloro and bromo), *p*-halobenzaldehyde and *p*-halobenzonitrile) have been used for the Suzuki reaction with phenylboronic acid. The targeted coupling reactions were achieved, under relatively mild experimental condition, in reasonably high yield (Table 2). For example, using 1 mol wt% of the Ni-catalyst, the Suzuki coupling between *p*-bromoacetophenone and phenylboronic acid was achieved in excellent yield (entry 1). However, while *p*-chloroacetophenone was used instead of *p*-bromoacetophenone, yield of the biphenyl product dropped to 62 wt% (entry 4). Besides, changing the para-substituent in the halobenzenes is also found to have significant influence on the yield of the biphenyl product (entries 1–3 and entries 4–6). We have also carried out the same coupling reaction in absence of catalyst (entry 7) and found <5% yield after 24 h which firmly establish the necessity of Ni catalyst to carryout Suzuki coupling reaction. The observed catalytic efficiency of these HPMC stabilized Ni nanoparticles, though not remarkably high, are found to be comparable to those found in the literature for similar nickel-catalyzed Suzuki

Table 2
Suzuki cross-coupling of aryl halides with phenylboronic acid.[a]

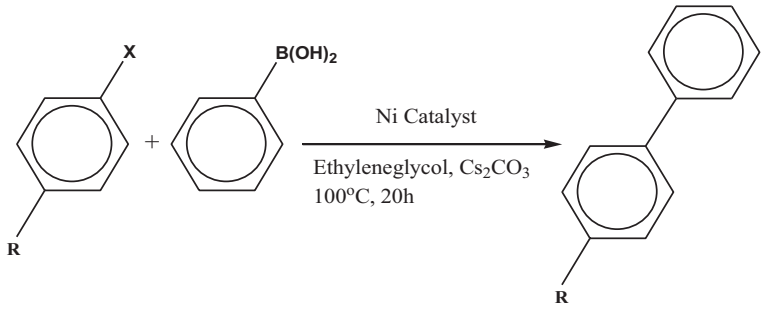

Entry	R	X	Conversion[b] (%)
1	COMe	Br	>99
2	CHO	Br	90
3	CN	Br	87
4	COMe	Cl	62
5	CHO	Cl	51
6	CN	Cl	44
7[c]	COMe	Br	<5

[a] Reaction composition: aryl halide (1.0 mmol), phenylboronic acid (1.2 mmol). Cs_2CO_3 (1.7 mmol), Ni-catalyst, solvent (4 mL).
[b] Determined by ^1H NMR on the basis of residual aryl halide (Albisson, Bedford, Noelle, & Lawrence, 1998; Chen, Liu, Peng, & Liu, 2005; Evans et al., 2005; Peris, Mata, Loch, & Crabtree, 2001).
[c] Reaction carried out in absence of catalyst.

coupling reactions. Also, it is a well known fact that polymer capped nanoparticles represent semi-heterogeneous catalytic system, as presence of polymer increases the interaction in the organic phase (Khurana & Vij, 2012). So, in addition to promoting enolization, HPMC stabilized Ni nanoparticles act as semi-heterogeneous high surface area catalyst and promote Suzuki type coupling reaction.

3.6. Typical procedure for the recycling of the Ni nanoparticles (catalyst)

Given the high efficacy of these nano-sized catalysts in the Suzuki-coupling reaction, their recyclability was then investigated as the separation and recycling of catalysts are still the key steps in heterogenous catalysis to ensure reusability and avoid undesired contamination in the final products. The nickel nanoparticles were easy to recover due to their good magnetic property. After the catalytic reaction, the reaction mixture was centrifuged and the Ni-nanoparticles were deposited as solid mass at the bottom of the centrifuge tube. The catalysts were reused after washing with absolute ethyl alcohol and treating under vacuum at 60 °C for 10 h. The same process was repeated after each reaction cycle to isolate and reuse the Ni-nanoparticles as catalyst. The present study shows that Ni nanoparticles have good catalytic properties in the Suzuki-coupling reaction and are easy to reuse.

4. Conclusion

The polymer coated fcc Ni nanoparticles have been synthesized using nickel chloride with hydrazine hydrate in presence of hydroxypropylmethylcellulose (HPMC) in mixed solvent of ethanol and triple distilled water via a simple and reliable one-pot reaction in an ambient atmosphere. The protective agent hydroxypropylmethylcellulose (HPMC) plays an important role to control the shape and size of polymer coated Ni nanoparticles. The synthesized Ni nanoparticles have been characterized by XRD, FTIR and FESEM analysis. A comparative study of structure and magnetic properties of HPMC stabilized and bare Ni nanoparticles have been carried out. The results of magnetic characterization showed that the polymer stabilized Ni nanoparticles exhibited quite different magnetic properties than those of the bare Ni nanoparticles. These resultant spherical Ni nanoparticles with high coercivity could be used as excellent high density magnetic recording materials. This method is simple, low cost and suitable for large-scale production of nanostructure Ni nanoparticles. Finally, it is concluded that the synthesized Ni nanoparticles shows excellent catalytic activity and recyclability toward Suzuki coupling reaction.

Acknowledgements

The authors D. Maity and S.K.N. gratefully acknowledge UGC, Govt. of India for providing fellowship. M.M.R.M. likes to thank DST for his fellowship under INSPIRE fellowship and D. Mondal thanks CSIR, New Delhi for his fellowship. We acknowledge CRNN-University of Calcutta for the magnetic measurement utilizing MPMS SQUID VSM.

References

Abdel-Aal, E. A., Malekzadeh, S. M., Rashad, M. M., El-Midany, A. A., & El-Shall, H. (2007). Effect of synthesis conditions on preparation of nickel metal nanopowders via hydrothermal reduction technique. *Powder Technology*, *171*, 63–68.
Albisson, D. A., Bedford, R. B., Noelle, S. P., & Lawrence, S. E. (1998). Orthopalladated triaryl phosphite complexes as highly active catalysts in biaryl coupling reactions. *Chemical Communications*, *19*, 2095–2096.
Alonso, F., Calvino, J. J., Osante, I., & Yus, M. (2005). A new straightforward and mild preparation of nickel (0) nanoparticles. *Chemistry Letters*, *34*, 1262–1263.
Alonso, F., Riente, P., & Yus, M. (2008a). Hydrogen-transfer reduction of carbonyl compounds promoted by nickel nanoparticles. *Tetrahedron*, *64*, 1847–1852.
Alonso, F., Riente, P., & Yus, M. (2008b). Hydrogen-transfer reduction of carbonyl compounds catalysed by nickel nanoparticles. *Tetrahedron Letter*, *49*, 1939–1942.
Alonso, F., Riente, P., & Yus, M. (2008c). Hydrogen-transfer reductive amination of aldehydes catalysed by nickel nanoparticles. *Synlett*, 1289–1292.
Bai, L., Yuan, F., & Tang, Q. (2008). Synthesis of nickel nanoparticles with uniform size via a modified hydrazine reduction route. *Materials Letters*, *62*, 2267–2270.
Brust, M., Walker, M., Bethell, D., Schiffrin, D. G., & Whyman, R. (1994). Synthesis of thiol-derivatised gold nanoparticles in a two-phase liquid–liquid system. *Journal of Chemical Society, Chemical Communication*, *7*, 801–802.
Carroll, K. J., Reveles, J. U., Shultz, M. D., Khanna, S. N., & Carpenter, E. E. (2011). Preparation of elemental Cu and Ni nanoparticles by the polyol method: An experimental and theoretical approach. *Journal of Physical Chemistry C*, *115*, 2656–2664.
Chen, C. L., Liu, Y. H., Peng, S. H., & Liu, S. T. (2005). Air- and moisture-stable cyclopalladated complexes as efficient catalysts for Suzuki–Miyaura coupling reaction. *Organometallics*, *24*, 1075–1081.
Chen, D. H., & Hsieh, C. H. (2002). Synthesis of nickel nanoparticles in aqueous cationic surfactant solutions. *Journal of Materials Chemistry*, *12*, 2412–2415.

Chen, D. H., & Wu, S. H. (2000). Synthesis of nickel nanoparticles in water-in-oil microemulsions. *Chemistry of Materials*, *12*, 1354–1360.
Chen, Y., Peng, D.-L., Lin, D., & Luo, X. (2007). Preparation and magnetic properties of nickel nanoparticles via the thermal decomposition of nickel organometallic precursor in alkylamines. *Nanotechnology*, *18*, 505703 (6 pp.).
Cordente, N., Amiens, C., Chaudret, B., Respaud, M., Senocq, F., & Casanove, M.-J. (2003). Chemisorption on nickel nanoparticles of various shapes: Influence on magnetism. *Journal of Applied Physics*, *94*, 6358–6365.
Cordente, N., Respaud, M., Senocq, F., Casanove, M. J., Amiens, C., & Chaudret, B. (2001). Synthesis and magnetic properties of nickel nanorods. *Nano Letter*, *1*, 565–568.
Couto, G. G., Klein, J. J., Schreiner, W. H., Mosca, D. H., de Oliveira, A. J. A., & Zarbin, A. J. G. (2007). Nickel nanoparticles obtained by a modified polyol process: Synthesis, characterization, and magnetic properties. *Journal of Colloid and Interface Science*, *311*, 461–468.
Dhakshinamoorty, A., & Pitchumani, K. (2008). Clay entrapped nickel nanoparticles as efficient and recyclable catalysts for hydrogenation of olefins. *Tetrahedron Letter*, *49*, 1818–1823.
Domínguez-Crespo, M. A., Ramírez-Meneses, E., Montiel-Palma, V., Torres Huerta, A. M., & Dorantes Rosales, H. (2009). Synthesis and electrochemical characterization of stabilized nickel nanoparticles. *International Journal of Hydrogen Energy*, *34*, 1664–1676.
Evans, P., Hogg, P., Grigg, R., Nurnabi, M., Hinsley, J., Sridharan, V., et al. (2005). 8-Methylquinoline palladacycles: Stable and efficient catalysts for carbon–carbon bond formation. *Tetrahedron*, *61*, 9696–9704.
Ferrando, R., Jellinek, J., & Johnston, R. L. (2008). Self-assembly of mesoporous Ni–B amorphous alloy catalysts. *Chemical Review*, *108*, 845–910.
Gao, J. Z., Guan, F., Zhao, Y. C., Yang, W., Ma, Y. J., Lu, X. Q., et al. (2001). Preparation of ultrafine nickel powder and its catalytic dehydrogenation activity. *Materials Chemistry and Physics*, *71*, 215–219.
Hernandez, R., Polizu, S., Turenne, S., & Yahia, L. (2002). Characteristics of porous nickel–titanium alloys for medical applications. *Bio-medical Materials and Engineering*, *12*, 37–45.
Hou, Y., & Gao, S. (2003). Monodisperse nickel nanoparticles prepared from a monosurfactant system and their magnetic properties. *Journal of Materials Chemistry*, *13*, 1510–1512.
Jiang, Z., Xie, J., Jiang, D., Jing, J., & Qin, H. (2012). Facile route fabrication of nano-Ni core mesoporous-silica shell particles with high catalytic activity towards 4-nitrophenol reduction. *CrystEngComm*, *14*, 4601–4611.
Jongen, N., Bowen, P., Lemaitre, J., Valmalette, J. C., & Hofmann, H. (2000). Precipitation of self-organized copper oxalate polycrystalline particles in the presence of hydroxypropylmethylcellulose (HPMC): Control of morphology. *Journal of Colloid and Interface Science*, *226*, 189–198.
Khurana, J. M., & Vij, K. (2012). Nickel nanoparticles: A highly efficient catalyst for one pot synthesis of tetraketones and biscoumarins. *Journal of Chemical Science*, *124*, 907–912.
Kim, K. H., Lee, Y. B., Choi, E. Y., Park, H. C., & Park, S. S. (2004). Synthesis of nickel powders from various aqueous media through chemical reduction method. *Materials Chemistry and Physics*, *86*, 420–424.
Kim, K. H., Park, H. C., Lee, S. D., Hwa, W. J., Hong, S. S., Lee, G. D., et al. (2005). Preparation of submicron nickel powders by microwave-assisted hydrothermal method. *Materials Chemistry and Physics*, *92*, 234–239.
Li, H. X., Zhao, Q. F., Wan, Y., Dai, W. L., & Qiao, M. H. (2006). Self-assembly of mesoporous Ni–B amorphous alloy catalysts. *Journal of Catalysis*, *244*, 251–254.
Li, Y., Cai, M., Rogers, J., Xu, Y., & Shen, W. (2006). Glycerol-mediated synthesis of Ni and Ni/NiO core–shell nanoparticles. *Materials Letters*, *60*, 750–753.
Li, Y. D., Li, C. W., Wang, H. R., Li, L. Q., & Qian, Y. T. (1999). Preparation of nickel ultrafine powder and crystalline film by chemical control reduction. *Materials Chemistry and Physics*, *59*, 88–90.
Ni, X., Zhang, J., Zhang, Y., & Zheng, H. J. (2007). Citrate-assisted synthesis of prickly nickel microwires and their surface modification with silver. *Journal of Colloid and Interface Science*, *307*, 554–558.
Ni, X. M., Zhang, Y. F., Song, J. M., & Zheng, H. G. (2007). Solvent mediated assembly of nickel crystallites: From chains to isolated spheres. *Journal of Crystal Growth*, *299*, 365–368.
Oliveira, M. M., Zanchet, D., Ugrate, D., & Zarbin, A. J. G. (2005). Influence of synthetic parameters on the size, structure, and stability of dodecanethiol-stabilized silver nanoparticles. *Journal of Colloid and Interface Science*, *292*, 429–435.
Park, J., Kang, E., Son, S. U., Park, H. M., Lee, M. K., Kim, J., et al. (2005). Monodisperse nanoparticles of Ni and NiO: Synthesis, characterization, self-assembled superlattices, and catalytic applications in the Suzuki coupling reaction. *Journal of Advanced Materials*, *17*, 429–434.
Peris, E., Mata, J., Loch, J. A., & Crabtree, R. H. (2001). Pd complex of a tridentate pincer CNC bis-carbene ligand as a robust homogenous Heck catalyst. *Chemical Communications*, 201–202.
Rashid, Md. H., Raula, M., & Mandal, T. K. (2011). Polymer assisted synthesis of chain-like cobalt–nickel alloy nanostructures: Magnetically recoverable and reusable catalysts with high activities. *Journal of Materials Chemistry*, *21*, 4904–4917.
Reiss, G., & Hütten, A. (2005). Magnetic nanoparticles: Applications beyond data storage. *Nature Materials*, *4*, 725–726.
Roy, A., Srinivas, V., Ram, S., De Toro, J. A., & Mizutani, U. (2005). Structure and magnetic properties of oxygen-stabilized tetragonal Ni nanoparticles prepared by borohydride reduction method. *Physical Review B*, *1*, 184443 (10 pp.).
Sadek, A. Z., Zhang, C., Hu, Z., Partridge, J. G., McCulloch, D. G., Wlodarski, W., et al. (2010). Uniformly dispersed Pt–Ni nanoparticles on nitrogen-doped carbon nanotubes for hydrogen sensing. *Journal of Physical Chemistry C*, *114*, 238–242.
Sahoo, S., Chakraborti, C., & Behra, P. K. (2012). Spectroscopic investigations of a ciprofloxacin/HPMC mucoadhesive suspension. *International Journal of Applied Pharmaceutics*, *4*, 1–8.
Sapkal, S. B., Shelke, K. F., Shingate, B. B., & Shingare, M. S. (2009). Nickel nanoparticle-catalyzed facile and efficient one-pot synthesis of polyhydroquinoline derivatives via Hantzsch condensation under solvent-free conditions. *Tetrahedron Letter*, *50*, 1754–1756.
Saxena, A., Kumar, A., & Mozumdar, S. (2007). Ni-nanoparticles: An efficient green catalyst for chemo-selective oxidative coupling of thiols. *Journal of Molecular Catalysis A: Chemical*, *269*, 35–40.
Shen, L., Laibinis, P. E., & Hatton, T. A. (1999). Bilayer surfactant stabilized magnetic fluids: Synthesis and interactions at interfaces. *Langmuir*, *15*, 447–453.
Singh, V., & Srinivas, V. (2010). Effect of polymer coating on the magnetic properties of oxygen-stabilized nickel nanoparticles. *Physical Review B*, *85*, 054417 (9 pp.).
Singla, M. L., Negi, A., Mahajan, V., Singh, K. C., & Jain, D. V. S. (2007). Catalytic behavior of nickel nanoparticles stabilized by lower alkyl ammonium bromide in aqueous medium. *Applied Catalysis A*, *323*, 51–57.
Stopic, S., Nedeljkovic, J., Rakocevic, Z., & Uskokovic, D. (1999). Influence of additives on the properties of spherical Ni particles prepared by ultrasonic spray pyrolysis. *Journal of Materials Research*, *14*, 3059–3065.
Van der Weerd, J., & Kazarian, S. G. (2005). Release of poorly soluble drugs from HPMC tablets studied by FTIR imaging and flow-through dissolution tests. *Journal of Pharmaceutical Science*, *94*, 2096–2109.
Wang, C., Zhang, X. M., Qian, X. F., Xie, Y., Wang, W. Z., & Qian, Y. T. (1998). Preparation of nanocrystalline nickel powders through hydrothermal-reduction method. *Materials Research Bulletin*, *33*, 1747–1751.
Wang, D. P., Sun, D. B., Yu, H. Y., & Meng, H. M. (2008). Morphology controllable synthesis of nickel nanopowders by chemical reduction process. *Journal of Crystal Growth*, *310*, 1195–1201.
Wu, S. H., & Chen, D. H. (2003). Synthesis and characterization of nickel nanoparticles by hydrazine reduction in ethylene glycol. *Journal of Colloid and Interface Science*, *259*, 282–286.
Wu, S. H., & Chen, D.-H. (2004). Synthesis and stabilization of Ni nanoparticles in a pure aqueous CTAB solution. *Chemistry Letters*, *33*, 406–407.
Wu, Z. J., Zhang, M. H., Zhao, Z. F., Li, W., & Tao, K. Y. (2008). Synthesis of a Pd on Ni–B nanoparticle catalyst by the replacement reaction method for hydrodechlorination. *Journal of Catalysis*, *256*, 323–330.
Yao, R., Xu, J., Lu, X., & Deng, S. (2011). Phase transition behavior of HPMC-AA and preparation of HPMC-PAA nanogels. *Journal of Nanomaterials*, 1–6, 507542.
Yu, K., Kim, D. J., Chung, H. S., & Liang, H. (2003). Dispersed rodlike nickel powder synthesized by modified polyol process. *Materials Letters*, *57*, 3992–3997.
Zach, M. P., & Penner, R. M. (2000). Nanocrystalline nickel nanoparticles. *Advanced Materials*, *12*, 878–883.
Zhang, D. E., Ni, X. M., Zheng, H. G., Li, Y., Zhang, X. J., & Yang, Z. P. (2005). Synthesis of needle-like nickel nanoparticles in water-in-oil microemulsion. *Materials Letters*, *59*, 2011–2014.
Zhang, H. T., Wu, G., Chen, X. H., & Qui, X. G. (2006). Synthesis and magnetic properties of nickel nanocrystals. *Materials Research Bulletin*, *41*, 495–501.